ILASS–Europe 2017, 28th Conference on Liquid Atomization and Spray Systems, 6-8 September 2017, Valencia, Spain
http://dx.doi.org/10.4995/ILASS2017.2017.4711

Weakly nonlinear instability of a viscous liquid jet

Marie-Charlotte Renoult[1], Günter Brenn[2,*], Innocent Mutabazi[3]
[1]CORIA, Université de Rouen, France
[2]ISW, Graz University of Technology, Austria
[3]LOMC, Université du Havre, France
*Corresponding author: guenter.brenn@tugraz.at

Abstract
A weakly nonlinear stability analysis of an axisymmetric viscous liquid jet is performed. The calculation is based on a small-amplitude perturbation method and restricted to second order. Contrary to the inviscid jet and the planar viscous sheet cases studied by Yuen in 1968 [1] and Yang et al. in 2013 [2], respectively, a part of the solution results from a polynomial approximation of Bessel functions. Results on interface shapes for a small wave number and initial perturbation amplitude, four different Ohnesorge numbers, taking into account the approximate part or not, are used to predict the influence of liquid viscosity on satellite drop formation and evaluate the influence of the approximation. It is observed that the liquid viscosity has a retarding effect on satellite drop formation, in agreement with previous experimental and numerical work. In addition, it is found that the approximate terms can be reasonably ignored, providing a simpler viscous weakly nonlinear model for the description of the first nonlinearity growth in liquid jets. The present work replaces the ILASS 2016 paper [3] by the authors on the same subject.

Keywords
Viscous liquid jet, nonlinear capillary instability, satellite drop formation.

Introduction
A liquid jet breaks up forming main and satellite drops. The present work is concerned with the influence of both liquid viscosity and nonlinearities on satellite drop formation.
The first linear stability analysis of the capillary instability of a liquid jet in an ambient medium was conducted by Rayleigh [4, 5], more than a century ago. In this reference work, the liquid is assumed inviscid and the ambient medium is the vacuum. His analysis shows that, in order to destabilize the jet, the wavelength λ of a varicose surface disturbance must be greater than the circumference of the undeformed circular jet cross section, as observed initially by Savart and Plateau [6, 7]. Two associated amplitude growth rates correspond to such an unstable perturbation wavelength, one being the opposite of the other, with the magnitude given by the well-known Rayleigh's linear dispersion relation for the inviscid jet in a vacuum.
The effect of liquid viscosity was then investigated by Weber [8], about fifty years later. The generalization of the previous dispersion relation introduces a growth rate and viscosity dependent modified wave number making the dispersion relation transcendental, yet numerically solvable, which is turned into a closed-form expression in the long-wave approximation. Contrary to the inviscid case, there are two different real growth rates with opposite signs for each unstable wavelength, with distinct absolute values below the corresponding inviscid one. This difference leads to dispersion relation curves always lower than the inviscid ones, as expected by the classical damping effect inferred from liquid viscosity.
Due to the linearity of the previous analysis, the interaction of disturbances with different wavelengths is not accounted for, and the drops produced by the jet breakup are predicted to be monodisperse in size. In particular, with no imposed perturbation, the most probable wavelength, i.e. the wavelength with maximum growth rate, is often used to get a good approximation for the main drop size in liquid jet breakup.
The effect of nonlinearities was first studied by Yuen [1]. In his weakly nonlinear analysis of an inviscid jet in a vacuum he described the jet interface shape up to order three at small initial deformation amplitude. Plotting jet surface profiles for various wave numbers and a fixed small initial amplitude perturbation, he observed the appearance of an undulation between the primary crests of the initial perturbation in the low wave number case. This observation is considered today as the first prediction of the formation of satellite drops. Good agreement of the predictions of his model with experimental results was found for the deviation of the jet surface shape from the single sinusoidal one [9], the satellite drop size [10, 11] and the growth rate of the two first nonlinear harmonics for wave numbers less than the fastest growing mode [12]. For larger wave numbers (more precisely, greater than the fastest growing mode), Yuen's model does not predict the formation of satellite drops, even though they are still observed in the experiment [10]. This stands as one limitation of the weakly nonlinear stability analysis.
Based on Yuen's model, the effect of liquid viscosity on the formation of drops was deduced. For inviscid jets, satellite drops are predicted to become smaller when the wave number converges to the fastest growing mode. With increasing viscosity, the fastest growing mode is shifted to lower wave numbers, and consequently the amplitude of the undulation is reduced, while its wavelength is increased, as pointed out by Goedde & Yuen [13]. This qualitative description is in agreement with experimental and numerical results showing that satellite drops can be completely suppressed for sufficiently high Ohnesorge numbers [14].
Recently, the effect of both liquid viscosity and nonlinearities was combined for the study of a liquid sheet, the planar counterpart of the axisymmetric jet, revealing a complicated influence of liquid viscosity on the nonlinear

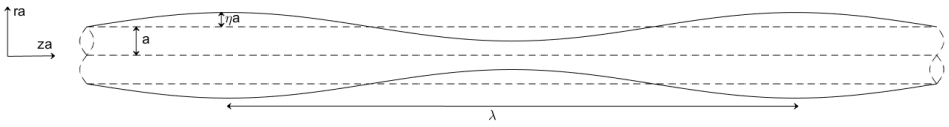

Figure 1. Sketch of the geometry of a capillary jet under varicose deformation.

sheet stability [2]. In a 2016 ILASS paper [3], the jet geometry was considered by the present authors, introducing the need for a polynomial approximation of one part of the viscous contribution, that could not be fully solved analytically, due to the presence of Bessel function products with different arguments. However, in this weakly nonlinear analysis, the two values of growth rates were incorrectly taken, as real numbers of the same absolute value but opposite signs, like in the inviscid case.
Here, we revisit our weakly nonlinear model of the temporal instability of a viscous jet in a vacuum to gain insight into the role of the jet liquid viscosity on satellite drop formation. The expansion of the jet interface shape is restricted to second order terms in the small initial perturbation amplitude, the second-order solution being sufficient to predict satellite drop formation [3]. In the following section we derive the equations of motion, as well as their boundary and initial conditions. Thereafter we solve the equations derived in the sequence of the order and present our method of approximation of one part of the viscous contribution containing products of Bessel functions with different arguments. Results on surface shapes are then presented and the effect of both the liquid viscosity and the level of approximation discussed by comparison to the inviscid solution of Yuen [1]. The paper ends with the conclusions.

Formulation of the problem

We study the weakly nonlinear temporal instability of a viscous liquid jet as sketched in Figure 1. The jet is assumed to be axisymmetric around the z axis of the cylindrical coordinate system. The liquid is treated as incompressible and Newtonian. The dynamic influence from the ambient air is neglected, i.e. we treat the ambience as a vacuum. Body forces are not accounted for, since Froude numbers are large. The problem is formulated in cylindrical coordinates to account for its geometry.
The flow variables and equations are adimensionalized with the undeformed jet radius a, the capillary time scale $(\rho a^3/\sigma)^{1/2}$ and the capillary pressure σ/a for length, time and pressure, respectively. Here, ρ is the liquid density and σ the air-liquid interfacial tension. The jet surface is described as a place where $r_s(t,z) = 1 + \eta(t,z)$, where η is the non-dimensional deformation against the undisturbed cylindrical shape (cf. Figure 1).
For the problem at hand, the equation of continuity and the two components of the momentum equation in the radial (r) and axial (z) directions read

$$\frac{1}{r}\frac{\partial}{\partial r}(ru_r) + \frac{\partial u_z}{\partial z} = 0 \tag{1}$$

$$\frac{\partial u_r}{\partial t} + u_r\frac{\partial u_r}{\partial r} + u_z\frac{\partial u_r}{\partial z} = -\frac{\partial p}{\partial r} + Oh\left[\frac{\partial}{\partial r}\left(\frac{1}{r}\frac{\partial}{\partial r}(ru_r)\right) + \frac{\partial^2 u_r}{\partial z^2}\right] \tag{2}$$

$$\frac{\partial u_z}{\partial t} + u_r\frac{\partial u_z}{\partial r} + u_z\frac{\partial u_z}{\partial z} = -\frac{\partial p}{\partial z} + Oh\left[\frac{1}{r}\frac{\partial}{\partial r}\left(r\frac{\partial u_z}{\partial r}\right) + \frac{\partial^2 u_z}{\partial z^2}\right] \tag{3}$$

where $Oh = \mu/(\sigma a\rho)^{1/2}$ is the Ohnesorge number, the characteristic dimensionless parameter distinguishing the viscous from the inviscid case, with the liquid dynamic viscosity μ. The closed set of the above equations must be solved subject to initial and boundary conditions. The kinematic boundary condition states that the material rate of deformation of the jet surface equals the radial velocity component at the place of the deformed surface. The kinematic boundary condition therefore reads

$$u_r = \frac{D\eta}{Dt} = \frac{\partial\eta}{\partial t} + u_z\frac{\partial\eta}{\partial z} \quad \text{at } r = 1+\eta \tag{4}$$

The first dynamic boundary condition states that the shear stress parallel to the jet surface is zero, since the ambient gas phase dynamic viscosity is very small, so that momentum cannot be transferred across the jet boundary at an appreciable rate. The second dynamic boundary condition states that the stress normal to the jet surface, composed from the flow-induced pressure and a viscous contribution, differs across the interface by the contribution due to the surface tension. The zero-shear stress boundary condition reads

$$(\vec{n}\cdot\tau)\times\vec{n} = \vec{0} \quad \text{at } r = 1+\eta \tag{5}$$

where the outward unit normal vector $\vec{n}$ is given as $\vec{n} = \left(\vec{e}_r - \frac{\partial\eta}{\partial z}\vec{e}_z\right)/\sqrt{1+\left(\frac{\partial\eta}{\partial z}\right)^2}$ and the viscous extra stress tensor τ in (5) is the one for the incompressible Newtonian fluid. The corresponding normal stress boundary condition reads

$$-p + Oh\,(\vec{n}\cdot\tau)\cdot\vec{n} + \left(\vec{\nabla}\cdot\vec{n}\right) = 0 \quad \text{at } r = 1+\eta \tag{6}$$

We obtain the divergence of the normal unit vector in this equation as

$$\left(\vec{\nabla}\cdot\vec{n}\right) = (1+\eta)^{-1}\left[1+\left(\frac{\partial\eta}{\partial z}\right)^2\right]^{-1/2} - \frac{\partial^2\eta}{\partial z^2}\left[1+\left(\frac{\partial\eta}{\partial z}\right)^2\right]^{-3/2} \quad \text{at } r=1+\eta \tag{7}$$

The initial surface disturbance is assumed to be purely sinusoidal with the amplitude η_0 and wave number $k = 2\pi a/\lambda$. With this assumption, volume conservation leads to the following expression for the initial non-dimensional jet shape [1]:

$$r_s(0,z) = 1+\eta(0,z) = \eta_0\cos kz + \left(1-\eta_0^2/2\right)^{1/2} = 1+\eta_0\cos kz - \frac{1}{4}\eta_0^2 - \frac{1}{32}\eta_0^4 - \dots \tag{8}$$

As usual in weakly nonlinear analysis, the initial deformation amplitude is assumed to be small, i.e. $\eta_0 \ll 1$.
For analyzing these equations in a weakly nonlinear form, the two velocity components and the pressure in the flow field, as well as the deformed interface shape, are expanded into power series with respect to the parameter η_0. This means that we formulate the dependencies as for, e.g., the radial velocity, pressure and jet shape:

$$u_r = u_{r1}\eta_0 + u_{r2}\eta_0^2 + \dots; \quad p = p_1\eta_0 + p_2\eta_0^2 + \dots; \quad r_s = 1+\eta_1\eta_0 + \eta_2\eta_0^2 + \dots \tag{9}$$

Furthermore, one important difference between the linear analysis and the present weakly nonlinear one is that the boundary conditions are satisfied on the deformed jet surface, not on the undeformed, circular cylindrical shape. For doing this, but still allowing for the functions in the boundary conditions to be evaluated on the undeformed jet surface, their values on the deformed shape are represented by Taylor expansions, such as

$$u_r|_{r=1+\eta} = u_r|_{r=1} + \left.\frac{\partial u_r}{\partial r}\right|_{r=1}\eta + \dots; \quad p|_{r=1+\eta} = p|_{r=1} + \left.\frac{\partial p}{\partial r}\right|_{r=1}\eta + \dots \tag{10}$$

Substituting these approaches into the flow equations (1) - (3) and into the boundary conditions (4), (5) and (6), and representing the flow properties and their derivatives as given in (9), we obtain sets of first and second order equations of motion with the boundary conditions consisting of all the terms with the deformation parameter η_0 to the first and second powers, respectively.

First-order equations

To obtain the first-order equations we collect all the terms in the above expansions with the parameter η_0 to the first power. The first-order continuity and momentum equations read

$$\frac{1}{r}\frac{\partial}{\partial r}(ru_{r1}) + \frac{\partial u_{z1}}{\partial z} = 0 \tag{11}$$

$$\frac{\partial u_{r1}}{\partial t} = -\frac{\partial p_1}{\partial r} + Oh\left[\frac{\partial}{\partial r}\left(\frac{1}{r}\frac{\partial}{\partial r}(ru_{r1})\right) + \frac{\partial^2 u_{r1}}{\partial z^2}\right] \tag{12}$$

$$\frac{\partial u_{z1}}{\partial t} = -\frac{\partial p_1}{\partial z} + Oh\left[\frac{1}{r}\frac{\partial}{\partial r}\left(r\frac{\partial u_{z1}}{\partial r}\right) + \frac{\partial^2 u_{z1}}{\partial z^2}\right] \tag{13}$$

For the boundary conditions of first order we obtain

$$u_{r1} = \frac{\partial\eta_1}{\partial t} \quad \text{at } r=1 \text{ kinematic} \tag{14}$$

$$\frac{\partial u_{z1}}{\partial r} + \frac{\partial u_{r1}}{\partial z} = 0 \quad \text{at } r=1 \text{ zero shear stress} \tag{15}$$

$$-p_1 + 2Oh\frac{\partial u_{r1}}{\partial r} - \left(\eta_1 + \frac{\partial^2\eta_1}{\partial z^2}\right) = 0 \quad \text{at } r=1 \text{ zero normal stress} \tag{16}$$

Furthermore, the initial conditions of first order are

$$\eta_1(0,z) = \cos kz \quad \text{and} \quad \frac{\partial\eta_1}{\partial t}(0,z) = 0 \tag{17}$$

Second-order equations

To obtain the second-order equations we collect all the terms in the above expansions with the parameter η_0 to the second power. The second-order continuity and momentum equations read

$$\frac{1}{r}\frac{\partial}{\partial r}(ru_{r2}) + \frac{\partial u_{z2}}{\partial z} = 0 \tag{18}$$

$$\frac{\partial u_{r2}}{\partial t} + u_{r1}\frac{\partial u_{r1}}{\partial r} + u_{z1}\frac{\partial u_{r1}}{\partial z} = -\frac{\partial p_2}{\partial r} + Oh\left[\frac{\partial}{\partial r}\left(\frac{1}{r}\frac{\partial}{\partial r}(ru_{r2})\right) + \frac{\partial^2 u_{r2}}{\partial z^2}\right] \tag{19}$$

$$\frac{\partial u_{z2}}{\partial t} + u_{r1}\frac{\partial u_{z1}}{\partial r} + u_{z1}\frac{\partial u_{z1}}{\partial z} = -\frac{\partial p_2}{\partial z} + Oh\left[\frac{1}{r}\frac{\partial}{\partial r}\left(r\frac{\partial u_{z2}}{\partial r}\right) + \frac{\partial^2 u_{z2}}{\partial z^2}\right] \tag{20}$$

The boundary conditions of second order at $r = 1$ are

$$u_{r2} = \frac{\partial \eta_2}{\partial t} + u_{z1}\frac{\partial \eta_1}{\partial z} - \eta_1 \frac{\partial u_{r1}}{\partial r} \quad \text{kinematic} \tag{21}$$

$$\frac{\partial u_{z2}}{\partial r} + \frac{\partial u_{r2}}{\partial z} + \eta_1 \frac{\partial}{\partial r}\left(\frac{\partial u_{z1}}{\partial r} + \frac{\partial u_{r1}}{\partial z}\right) + 2\left(\frac{\partial u_{r1}}{\partial r} - \frac{\partial u_{z1}}{\partial z}\right)\frac{\partial \eta_1}{\partial z} = 0 \quad \text{zero shear stress} \tag{22}$$

$$-p_2 - \eta_1 \frac{\partial p_1}{\partial r} + 2Oh\left[\eta_1 \frac{\partial^2 u_{r1}}{\partial r^2} + \frac{\partial u_{r2}}{\partial r} - \frac{\partial \eta_1}{\partial z}\left(\frac{\partial u_{z1}}{\partial r} + \frac{\partial u_{r1}}{\partial z}\right)\right] - \left[\eta_2 + \frac{\partial^2 \eta_2}{\partial z^2} + \frac{1}{2}\left(\left(\frac{\partial \eta_1}{\partial z}\right)^2 - 2\eta_1^2\right)\right] = 0 \quad \text{zero normal stress} \tag{23}$$

Furthermore, the initial conditions of second order are

$$\eta_2(0, z) = -1/4 \quad \text{and} \quad \frac{\partial \eta_2}{\partial t}(0, z) = 0 \tag{24}$$

Solving these sets of equations will reveal the weakly nonlinear role of the viscous stresses in the jet liquid on the capillary instability of a Newtonian viscous liquid jet in a vacuum.

Solutions of the governing equations

First-order solutions

The first-order equations describe the linear problem. They exhibit well known solutions expected to be recovered by our equations. In particular, we expect to recover the special form of the dispersion relation of the viscous jet first presented by Weber [8] without the ambient gas influence.

Since we are looking at two-dimensional flow fields, for determining the first-order velocity and pressure fields we apply the method of the Stokesian stream function. The stream function ψ represents the liquid motion due to the disturbance from the cylindrical form of the jet. The stream function is defined by its relations to the two velocity components u_{r1} and u_{z1} as per [15]

$$u_{r1} = -\frac{1}{r}\frac{\partial \psi}{\partial z} \quad , \quad u_{z1} = \frac{1}{r}\frac{\partial \psi}{\partial r} \tag{25}$$

Using this definition of the velocity components as derivatives of the stream function, the resulting first-order velocity field satisfies the continuity equation identically.

The first-order interface deformation is assumed to remain sinusoidal. η_1 is thus searched under the form

$$\eta_1 = \hat{\eta}_1 \exp\left(ikz - \alpha_1 t\right) \tag{26}$$

with α_1 the first-order angular frequency of the jet problem.

Taking the curl of the momentum equation in a vector form based on (12) and (13), we obtain the equation

$$\left(\frac{1}{Oh}\frac{\partial}{\partial t} - E^2\right)\left(E^2 \psi\right) = 0, \quad \text{where} \quad E^2 = r\frac{\partial}{\partial r}\left(\frac{1}{r}\frac{\partial}{\partial r}\right) + \frac{\partial^2}{\partial z^2} \tag{27}$$

for the stream function. The solution of (27) for a flow field containing the position $r = 0$ reads [16]

$$\psi(r, z, t) = \left[C_1 r I_1(kr) + C_3 r I_1(lr)\right] \exp\left(ikz - \alpha_1 t\right) \tag{28}$$

where $l^2 = k^2 - \alpha_1/Oh$. The two constants C_1 and C_3 are determined by the kinematic and the dynamic zero tangential stress boundary conditions (14) and (15) and read

$$C_1 = -\frac{i\alpha_1 \hat{\eta}_1}{kI_1(k)}\frac{l^2 + k^2}{l^2 - k^2} = \frac{i\hat{\eta}_1}{kI_1(k)}\left(2k^2 Oh - \alpha_1\right), \quad C_3 = \frac{i2\alpha_1 \hat{\eta}_1}{I_1(l)}\frac{k}{l^2 - k^2} = -\frac{i2\hat{\eta}_1 Oh\, k}{I_1(l)} \tag{29}$$

With these constants, the stream function of the disturbance is known, but the angular frequency α_1 remains to be determined. From the stream function we may calculate the velocity field in the jet due to the disturbance as

$$u_{r1} = -ik\left[C_1 I_1(kr) + C_3 I_1(lr)\right] \exp\left(ikz - \alpha_1 t\right) \tag{30}$$

$$u_{z1} = \left[C_1 k I_0(kr) + C_3 l I_0(lr)\right] \exp\left(ikz - \alpha_1 t\right) \tag{31}$$

The pressure due to the disturbance in the liquid field is obtained by integrating one component of the momentum equation. For this, the z component is the right choice since it offers an easy integration with respect to the z coordinate. The result is

$$p_1 = -i\alpha_1 C_1 I_0(kr) \exp\left(ikz - \alpha_1 t\right) + f(t, r) \tag{32}$$

where $f(t,r)$ must be equal to zero to satisfy the boundary condition (16). The dispersion relation of the jet is now found by introducing the velocity field and the pressure in the jet into the dynamic zero normal stress boundary condition (16). The result is the well-known relation

$$\alpha_1^2 - 2\alpha_1 k^2 Oh \left[1 - \frac{1}{k}\frac{I_1(k)}{I_0(k)} - \frac{2kl}{l^2+k^2}\frac{I_1(k)}{I_0(k)}\left(\frac{I_0(l)}{I_1(l)} - \frac{1}{l}\right)\right] = k\left(1-k^2\right)\frac{I_1(k)}{I_0(k)}\frac{l^2-k^2}{l^2+k^2} \tag{33}$$

which was first presented by Weber [8]. For zero liquid viscosity $(Oh \to 0)$, this relation reduces to the result of Rayleigh [4] for the inviscid jet in a vacuum.
For disturbance wave numbers $0 \le k \le 1$, the relation (33) has two real solutions α_1^+ and α_1^-, one positive and one negative, where, due to the formulation of the time dependency by the exponential function, the unstable behaviour of the jet is associated with the negative one. Note that this is the main point of difference from our previous version of the analysis [3], where the two solutions were incorrectly assumed to be of same absolute value like in the inviscid case. For wave numbers $k > 1$, the relation has two conjugate complex roots with a positive real part. The two values of α_1 represent two waves on the jet surface travelling in different directions and with different phase velocity. Accounting for both these waves, we formulate the first-order jet surface shape as

$$\eta_1(z,t) = \hat{\eta}_1^+ \exp\left(ikz - \alpha_1^+ t\right) + \hat{\eta}_1^- \exp\left(ikz - \alpha_1^- t\right) \tag{34}$$

The first-order initial conditions (17) require that initially the jet surface is governed by the function $\cos kz$ and is at rest. For the amplitudes $\hat{\eta}_1^+$ and $\hat{\eta}_1^-$ these conditions reveal the equations

$$\hat{\eta}_1^+ = -\frac{\alpha_1^-}{\alpha_1^+ - \alpha_1^-} \quad \text{and} \quad \hat{\eta}_1^- = \frac{\alpha_1^+}{\alpha_1^+ - \alpha_1^-} \tag{35}$$

so that the amplitudes are known. The first-order stream function, velocity components and pressure are then obtained. As an example, the radial velocity component reads

$$\begin{aligned} u_{r1}(r,z,t) &= \hat{\eta}_1^+ \left[\left(2k^2 Oh - \alpha_1^+\right)\frac{I_1(kr)}{I_1(k)} - 2k^2 Oh \frac{I_1(l^+ r)}{I_1(l^+)}\right]\exp\left(ikz - \alpha_1^+ t\right) + \\ &+ \hat{\eta}_1^- \left[\left(2k^2 Oh - \alpha_1^-\right)\frac{I_1(kr)}{I_1(k)} - 2k^2 Oh \frac{I_1(l^- r)}{I_1(l^-)}\right]\exp\left(ikz - \alpha_1^- t\right) \\ &=: \hat{\eta}_1^+ f_r^+(r)\exp\left(ikz - \alpha_1^+ t\right) + \hat{\eta}_1^- f_r^-(r)\exp\left(ikz - \alpha_1^- t\right) \end{aligned} \tag{36}$$

where the modified wave number l appearing in the coefficients C_1 and C_3 was formulated with the two different values of α_1 and denoted with the superscripts corresponding to their signs. And analogously, the axial velocity component reads:

$$u_{z1}(r,z,t) =: i\hat{\eta}_1^+ f_z^+(r)\exp\left(ikz - \alpha_1^+ t\right) + i\hat{\eta}_1^- f_z^-(r)\exp\left(ikz - \alpha_1^- t\right) \tag{37}$$

For zero liquid viscosity, as already stressed, the two solutions of α_1 exhibit the same absolute value, but have different signs. Furthermore the two amplitudes of the first-order jet surface shape in (35) assume the same value of $1/2$. The two velocity components, pressure and jet surface shape therefore reduce to the inviscid solutions by Yuen [1]. E.g., the inviscid first-order radial velocity component and pressure read

$$u_{r1,0}(r,z,t) = \alpha_1 \frac{I_1(kr)}{I_1(k)} exp\,(ikz)\sinh\alpha_1 t; \quad p_{1,0}(r,z,t) = -\alpha_1^2 \frac{I_0(kr)}{kI_1(k)} exp\,(ikz)\cosh\alpha_1 t \tag{38}$$

This serves as a validation of the first-order viscous solution. The respective real solutions arise by reducing the exponential functions $exp(ikz)$ to their real parts.

Second-order solutions

We now proceed to the second-order equations. e.g., the second-order solutions for the radial velocity component and the jet surface shape are sought under the forms

$$\begin{aligned} u_{r2}(r,z,t) &= u_{r21}^+(r)e^{2ikz-2\alpha_1^+ t} + u_{r21}^-(r)e^{2ikz-2\alpha_1^- t} + u_{r21}^{\pm}(r)e^{2ikz-(\alpha_1^+ + \alpha_1^-)t} + \\ &+ u_{r22}^p(r)e^{2ikz-\alpha_2^p t} + u_{r22}^m(r)e^{2ikz-\alpha_2^m t} \end{aligned} \tag{39}$$

$$\begin{aligned} \eta_2(z,t) &= \hat{F}_{21}^+ e^{2ikz-2\alpha_1^+ t} + \hat{G}_{21}^+ e^{-2\alpha_1^+ t} + \hat{F}_{21}^- e^{2ikz-2\alpha_1^- t} + \hat{G}_{21}^- e^{-2\alpha_1^- t} + \\ &+ \hat{F}_{21}^{\pm} e^{2ikz-(\alpha_1^+ + \alpha_1^-)t} + \hat{G}_{21}^{\pm} e^{-(\alpha_1^+ + \alpha_1^-)t} + \hat{\eta}_{22}^p e^{2ikz-\alpha_2^p t} + \hat{\eta}_{22}^m e^{2ikz-\alpha_2^m t} \end{aligned} \tag{40}$$

These forms result from the mathematical structures of the second-order equations of motion (18) - (20), with the nonlinear terms of first order involved, and the boundary conditions (21) - (23). We look at wave numbers $k < 1$ yielding linear instability.
The various contributions to the second-order solutions are now determined. Looking at the second-order equations of motion (18) - (20) we see that it is convenient to eliminate the second-order velocities from the momentum

equations using the continuity equation (18) to obtain a differential equation for the second-order pressure p_{21}. The result is the equation

$$\Delta p_{21} = -\mathrm{div}\left[\left(\vec{v}_1 \cdot \vec{\nabla}\right)\vec{v}_1\right] \tag{41}$$

In this equation $\vec{v}_1$ represents the first-order velocity field. Using the Lamé identity for the convective derivative of $\vec{v}_1$, (41) becomes

$$\Delta\left[p_{21} + \vec{v}_1^2/2\right] = +\mathrm{div}\left[\vec{v}_1 \times \left(\vec{\nabla} \times \vec{v}_1\right)\right] \tag{42}$$

This is a Poisson equation for the total pressure $\mathcal{P}_{21} := p_{21} + \vec{v}_1^2/2$. The structure of the solution in terms of its dependency on the axial coordinate and on time is determined by $\vec{v}_1^2/2$ and by the terms on the right of (42). Both groups of terms contain exponential functions of twice the two rates of growth or decay, $-2\alpha_1^+$ and $-2\alpha_1^-$, and the sum of the two rates, $-(\alpha_1^+ + \alpha_1^-)$, each multiplied by time. In view of the limited space, we present the terms depending on $exp(-2\alpha_1^+ t)$ only. The others are derived analogously. Using the representation of the stream function by modified Bessel functions, we re-write (42) and obtain the form

$$\begin{aligned}\Delta\left[\mathcal{P}_{21}^+\right] &= \frac{l^{+\,2} - k^2}{r^2}\left\{C_3^{+\,2}\left[\left(l^{+\,2} - 2k^2\right) r^2 I_1^2(l^+ r) + l^{+\,2} r^2 I_0^2(l^+ r)\right] + \right. \\ &+ \left. C_1^+ C_3^+\left[k r l^+ r I_0(kr) I_0(l^+ r) - k^2 r^2 I_1(kr) I_1(l^+ r)\right]\right\} e^{2ikz - 2\alpha_1^+ t}\end{aligned} \tag{43}$$

for the dependency of time represented here. The solutions may be composed from the general solutions of the homogeneous equations and the particular solutions of the inhomogeneous equations. The final form of the solution, formulated for the pressure contribution p_{21}^+, reads

$$p_{21}^+(r,z,t) = \left\{\left[-\frac{1}{4}\,\hat{\eta}_1^{+\,2}\left(f_r^{+\,2} - f_z^{+\,2}\right) + C_{21}^+ I_0(2kr) + \sum_{i=1}^{I}\delta_{2i}^+ r^{2i}\right] e^{2ikz} + \left[\hat{P}_{21}^+ + \frac{1}{4}\,\hat{\eta}_1^{+\,2}\left(f_r^{+\,2} + f_z^{+\,2}\right)\right]\right\} e^{-2\alpha_1^+ t}$$

where the coefficients $\delta_{2i}^+(k, l^+, C_1^+, C_3^+, q_{2i})$ arise from a polynomial approximation at order I of the Bessel functions in the right-hand side of equation (43) according to $I_{0,I}(x) = \sum_{i=1}^{I} q_{2(i-1)} x^{2(i-1)}$ and $I_{1,I}(x) = I'_{0,I}(x)$. From the second-order pressure field and the equations of motion (18) and (19), the corresponding second-order contributions to the two velocity components are determined. The differential equation (19) for u_{r2} yields the solution

$$u_{r21}^+ = \left\{D_{21}^+ I_1(2m^+ r) + \frac{kC_{21}^+}{\alpha_1^+} I_1(2kr) + \sum_{i=1}^{I-1}\zeta_{2i+1}^+ r^{2i+1}\right\} e^{2ikz - 2\alpha_1^+ t} \tag{44}$$

where $m^{+\,2} = k^2 - \alpha_1^+/(2Oh)$ and the coefficients $\zeta_{2i}^+(k, l^+, m^+, C_1^+, C_3^+, Oh, q_{2i})$ again arise from approximations of the Bessel functions in the right-hand side of the radial velocity component differential equation (not reported here). From the velocity u_{r21} and the continuity equation (18), the contributions to u_{z21} are determined easily. The part depending on $exp(-2\alpha_1^+ t)$ reads

$$u_{z21}^+ = \frac{i}{2k}\left\{D_{21}^+ 2m^+ I_0(2m^+ r) + \frac{2kC_{21}^+}{\alpha_1^+} I_0(2kr) + \sum_{i=1}^{I-1} 2(i+1)\zeta_{2i+1}^+ r^{2i}\right\} e^{2ikz - 2\alpha_1^+ t} \tag{45}$$

The coefficients C_{21}^+ and D_{21}^+, as well as the amplitudes $\hat{P}_{21}^+$, $\hat{F}_{21}^+$ and $\hat{G}_{21}^+$ (see equation (40)) are unknown constants, which are determined using the three boundary conditions of the second-order problem. The terms depending on $exp(-2\alpha_1^- t)$ and $exp(-(\alpha_1^- + \alpha_1^+)t$, and thus the amplitudes $\hat{P}_{21}^-$, $\hat{F}_{21}^-$, $\hat{G}_{21}^-$, $\hat{P}_{21}^\pm$, $\hat{F}_{21}^\pm$, $\hat{G}_{21}^\pm$ are obtained following the same method.

The second parts of the second-order solutions, with subscripts 22, which depend on time through the frequency α_2 of the second-order problem, are directly deduced from the equations for the linear problem, since they are of the same structure as for first order, with the wave number k replaced by $2k$, the angular frequency α_1 by α_2, and the deformation amplitude $\hat{\eta}_1$ by $\hat{\eta}_{22}$. The frequency α_2 is therefore obtained as a solution of a dispersion relation which is formally equal to the first order relation (33), but formulated with double the wave number. The only unknown remaining is therefore the amplitude $\hat{\eta}_{22}$. e.g., the equation for the radial velocity component with subscripts 22 read

$$\begin{aligned}u_{r22}(r,z,t) &= \hat{\eta}_{22}^p\left[\left(8k^2 Oh - \alpha_2^p\right)\frac{I_1(2kr)}{I_1(2k)} - 8k^2 Oh\frac{I_1(m_2^p r)}{I_1(m_2^p)}\right]\exp\left(2ikz - \alpha_2^p t\right) + \\ &+ \hat{\eta}_{22}^m\left[\left(8k^2 Oh - \alpha_2^m\right)\frac{I_1(2kr)}{I_1(2k)} - 8k^2 Oh\frac{I_1(m_2^m r)}{I_1(m_2^m)}\right]\exp\left(2ikz - \alpha_2^m t\right)\end{aligned} \tag{46}$$

where we have defined $m_2^2 = 4k^2 - \alpha_2/Oh$ and denote the two solutions of the dispersion relation for α_2 by superscripts p and m, since they may be either real or (conjugate) complex, depending on the wave number k. In the case of the real solutions, the superscripts denote the positive and negative values, and for the complex solutions they denote the positive and negative imaginary parts. The real part is positive for all the wave numbers

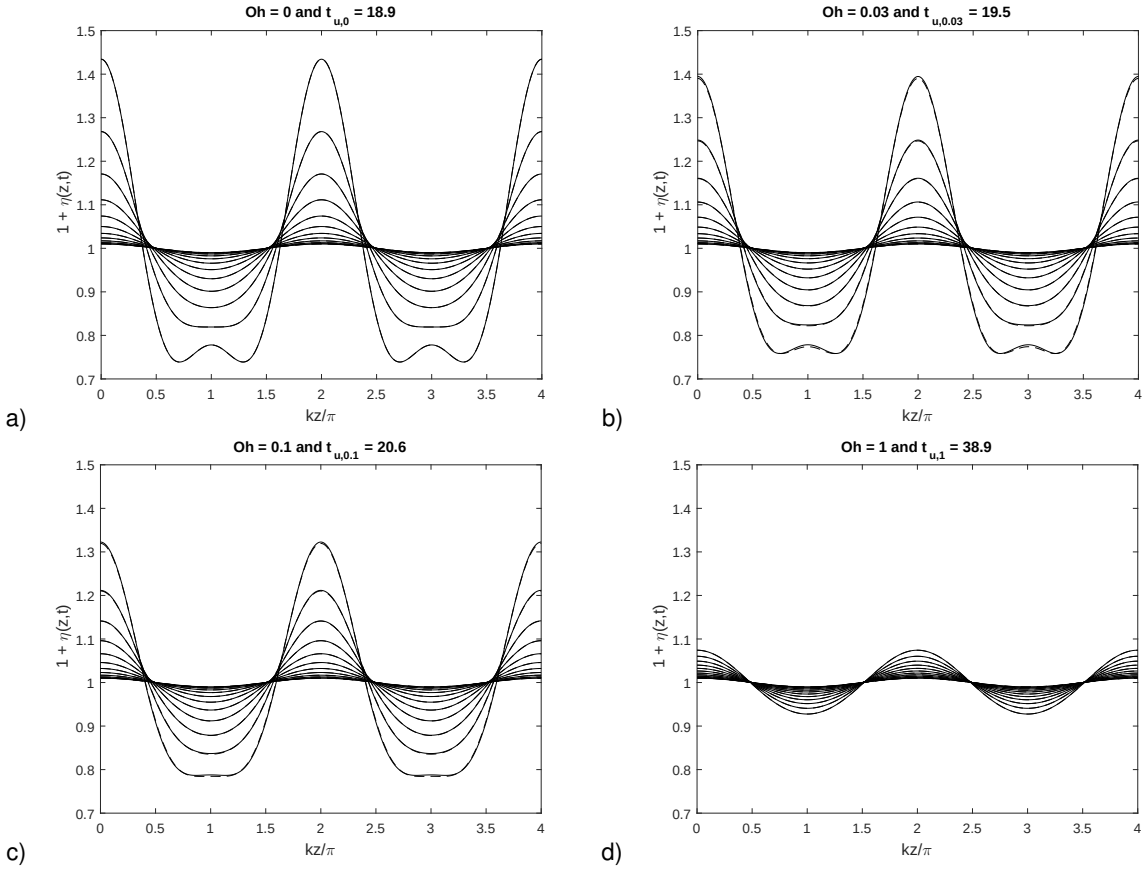

Figure 2. Surface shapes for various Ohnesorge numbers: a) $Oh = 0$ (inviscid case), b) $Oh = 0.03$, c) $Oh = 0.1$, d) $Oh = 1$ for discrete times $t = [0, \Delta t, 2\Delta t, \ldots, t_u, t_u + \Delta t]$ with $\Delta t = t_u/10$. The value of t_u is indicated in each figure. Disturbance wave number $k = 0.3$ and initial deformation amplitude $\eta_0 = 0.01$. Lines are drawn as solid for surface shapes taking into account the approximate viscous contribution with $I = 6$ and as dashed for neglecting it.

$1 \leq 2k \leq 2$. The values of $\hat{\eta}_{22}^p$ and $\hat{\eta}_{22}^m$ are deduced from the two initial conditions. From the first-order and second-order contributions we finally construct the description of the velocity components, the pressure, and the deformed jet surface to second order as defined in Eq. (9). For example, the deformed jet surface to second order reads:

$$r_s(z,t) \quad = \quad 1 + \eta(z,t) = 1 + \eta_0\eta_1(z,t) + \eta_0^2\eta_2(z,t) \tag{47}$$

where

$$\eta_1(z,t) \quad = \quad \left(\hat{\eta}_1^+ \; e^{-\alpha_1^+ t} + \hat{\eta}_1^- \; e^{-\alpha_1^- t}\right) \cos kz \tag{48}$$

and

$$\eta_2(z,t) \quad = \quad \frac{1}{2}\left(\hat{\eta}_{22}^p \; e^{-\alpha_2^p t} + \hat{\eta}_{22}^m \; e^{-\alpha_2^m t} + \hat{F}_{21}^+ \; e^{-2\alpha_1^+ t} + \hat{F}_{21}^- \; e^{-2\alpha_1^- t} + \hat{F}_{21}^{\pm} \; e^{-\left(\alpha_1^- + \alpha_1^+\right)t}\right) \; \cos 2kz + \tag{49}$$

$$- \quad \frac{1}{4} \; e^{-2\left(\alpha_1^- + \alpha_1^+\right)t} \left(\hat{\eta}_1^- \; e^{\alpha_1^+ t} + \hat{\eta}_1^+ \; e^{\alpha_1^- t}\right)^2 \tag{50}$$

The problem of second-order weakly nonlinear viscous jet instability is thus fully solved. From our above equations, the inviscid solution of Yuen [1] is retrieved for zero liquid viscosity $(Oh \to 0)$.

Results and discussion

With the presently developed viscous weakly nonlinear model, the influence of viscosity on the phenomenon of satellite drop formation is investigated. Satellite drop formation is here identified by the appearance of an undulation, i.e., a local maximum between two consecutive crests, prior to jet breakup $(\eta = -1)$. Based on the second-order representation of the jet surface in (47), the undulation occurs as soon as $4\eta_2\eta_0/\eta_1 = 1$. We denote the time for which the previous relation is satisfied as t_u. Like in the inviscid case [1], the undulation is not predicted for wave numbers greater than the fastest growing mode. Since the latter decreases with increasing liquid viscosity, a relatively small value of k is selected to allow for comparison between different values of the Ohnesorge number. The initial deformation amplitude is imposed too, since its influence on the jet surface wave does not depend on the liquid viscosity and has already been studied by Yuen [1]. Jet surface shapes are thus calculated for a fixed wave number $k = 0.3$ and initial deformation amplitude $\eta_0 = 0.01$.

In Figure 2, jet surface shapes are drawn at different times for four selected Ohnesorge numbers: 0 (inviscid case), 0.03, 0.1 and 1. For all these values, the non-dimensional fastest growing mode, given as $[2\,(1+3Oh)]^{-1/2}$ by the long-wave approximation [8], remains greater than 0.3, which means that the formation of an undulation is expected by the viscous model. For each case, the time increment between two consecutive shapes is $\Delta t = t_u/10$, the first time is 0 and the last time is $t_u + \Delta t$. Solid lines represent the viscous solutions for which the approximate terms are considered up to order $I = 6$, whereas dashed lines correspond to the solutions for which the approximate terms are omitted.
The comparison between jet surfaces drawn for different Ohnesorge numbers reveals a retarding effect of the jet liquid viscosity on the apparition of the undulation. This is in agreement with experimental [13] and numerical [14] results, where it is found that satellite droplets are fewer with jets of more viscous liquids. Moreover, the comparison between solutions of different levels of approximation shows that the solution neglecting the viscous term on the right-hand side of equation (42) is enough to represent the jet surface shape for the wave number investigated. This result allows us to simplify the viscous model by ignoring the approximate terms.
These first results will be completed in the next future by considering the effect of the surrounding ambient medium and liquid viscoelasticity.

Conclusions

A weakly nonlinear stability analysis of a viscous Newtonian liquid jet in a vacuum was performed. By including the viscous stresses in the liquid, the model complements the results of Yuen [1] for the inviscid case and Yang and co-authors [2] for a plane viscous liquid sheet. In a weakly nonlinear analysis, velocity, pressure and jet surface shape are expanded in series with respect to a small deformation parameter, here the initial amplitude of the jet deformation, yielding a set of equations with different powers of the parameter. Our analysis is restricted to second order for the sake of simplicity, in a first attempt to solve the viscous jet problem. The first-order solution corresponds to the linear one first derived by Weber [8] which converges to Rayleigh's solution for the inviscid case [4]. The second-order solution represents the nonlinear influence from the first-order fields and is obtained by solving a Poisson equation for the second-order pressure field. A polynomial approximation was used to take into account the viscous terms on the right hand side of this equation, leading to a viscous model with an approximation representing a part of the viscous influence. At vanishing Ohnesorge number of the jet, our equations reduce to Yuen's inviscid results [1]. Varying the jet Ohnesorge number between 0.03 and 1 reveals a retarding effect of the viscosity on the formation of the undulation, thus on satellite drop formation in liquid jet breakup. This is in agreement with the experiment [13, 17]. The influence of the level of approximation was also explored by comparing the solutions with and without the approximate part. The results suggest that the approximate part can be ignored, thus yielding a simpler viscous weakly nonlinear model of capillary liquid jet instability. The analysis will be carried further to include the influence from a gaseous ambient medium and viscoelastic liquid behaviour.

Acknowledgements

G.B. is indebted to I.M. and his team at the LOMC of the CNRS in Le Havre, and to Christophe Dumouchel at CORIA in Rouen, for their hospitality during three sabbatical stays in September 2014, September 2015, and December 2016 and acknowledges the inspiring atmospheres at the two laboratories. MC.R. was supported by the LABEX EMC^3 under the project TUVECO.

References

[1] Yuen, M.C., 1968, *J. Fluid Mech.*, 33, pp. 151-163.
[2] Yang, L. J., Wang, C., Fu, Q. F., Du, M. L., Tong, M. X., 2013, *J. Fluid Mech.*, 735, pp. 249-287.
[3] Renoult, M. C., Brenn, G., Mutabazi, I., 2016, *ILASS 2016*.
[4] Rayleigh, J.W.S. Lord, 1878, *Proc. London Mathematical Society*, 10, pp. 4-13.
[5] Rayleigh, J.W.S. Lord, 1879, *Proc. Royal Society London A*, 29, pp. 71-97.
[6] Savart, F., 1833, *Annales de Chimie et Physique*, 53, pp. 337-386.
[7] Plateau, J., 1873, *Gauthiers-Villars, Paris*, pp. 450-495.
[8] Weber, C., 1931, *Zeitschrift für Angewandte Mathematik und Mechanik*, 11, pp. 136-154.
[9] Rutland, D.F., Jameson, G.J., 1971, *J. Fluid Mech.*, 46, pp. 267-271.
[10] Rutland, D.F., Jameson, G.J., 1970, *Chemical Engineering Science*, 25, pp. 1689-1698.
[11] Lafrance, P., 1975, *Physics of Fluids*, 18, pp. 428-432.
[12] Taub, H.H., 1976, *Physics of Fluids*, 19, pp. 1124-1129.
[13] Goedde, E.F., Yuen, M.C., 1970, *J. Fluid Mech.*, 40, pp. 495-511.
[14] Ashgriz, N., Mashayek, F., 1995, *J. Fluid Mech.*, 291, pp. 163-190.
[15] Bird, R.B., Stewart, W.E., Lightfoot, E.N., 1960, "Transport Phenomena". J. Wiley and Sons, New York.
[16] Brenn, G., 2017, "Analytical solutions for transport processes". Springer, Heidelberg, New York.
[17] Brenn, G., Frohn, A., 1993, *Experiments in Fluids*, 15, pp. 85-90.